# Synthesis, Spectroscopy and Photophysical Properties of Ruthenium Triazole Complexes and Their Application as Dye-Molecules in Regenerative Solar Cells

**Anthea C. Lees,[a] Bénédicte Evrard,[a] Tia E. Keyes,[a,b] Johannes G. Vos,[a] Cornelis J. Kleverlaan,*[c] Monica Alebbi,[c] and Carlo A. Bignozzi[c]**

**Keywords:** Ruthenium / Triazole / Titanium / Electron Transfer / Sensitizers

The complexes $[Ru(dcb)_2(L)]$ {L = 3-(2-hydroxyphenyl)-5-(pyridin-2-yl)-1,2,4-triazole (2-ppt), 3-(4-hydroxyphenyl)-5-(pyridin-2-yl)-1,2,4-triazole (4-ppt), 3,5-bis(pyrazin-2-yl)-1,2,4-triazole (bpzt), 3-(2-hydroxyphenyl)-5-(pyrazin-2-yl)-1,2,4-triazole (2-ppzt) and dcb = 4,4′-$(CO_2H)_2$-2,2′-bipyridine} have been synthesized, spectroscopically characterized and anchored to nanocrystalline $TiO_2$ electrodes for the conversion of light into electricity in regenerative solar cells. The different efficiencies observed have been rationalized on the basis of an analytical expression relating the incident photon-to-current conversion efficiency (IPCE) to the kinetic parameters of the relevant electron transfer processes involved in the solar cell.

## Introduction

In the search for new solar energy conversion systems, dye-sensitized wide bandgap semiconductors have attracted much attention.[1−14] Solar cells containing photoanodes based on highly porous nanocrystalline $TiO_2$ films with adsorbed ruthenium dyes have demonstrated photon-to-current conversion efficiencies in the range 7−10% at AM 1.5.[6,12,15,16] The general mechanism of sensitization in a regenerative dye solar cell is shown in Scheme 1.[10,17,18] Excitation of an adsorbed dye molecule (D*) is followed by electron injection ($k_2$) to the semiconductor conduction band (CB). The oxidized dye molecule is reduced by an electron donor ($k_4$), which is present in the electrolyte. Reduction of the oxidized dye molecule ($D^+$) takes place via the sacrificial donor $I^-$, which is regenerative at the counterelectrode ($k_7$) ($Pt/SnO_2$). Losses in efficiency can occur by radiative and nonradiative decay of the excited state ($k_1$), by recombination of electrons in $TiO_2$ with oxidized dye molecules ($k_3$), and by electrons in $TiO_2$ which react with oxidants in solution ($k_6$).

Measuring the monochromatic incident photon-to-current efficiency, IPCE, gives the overall efficiency of the processes involved in the photovoltaic cell. IPCE is directly related to the absorption characteristics of the dye, the surface coverage of the $TiO_2$ electrode (LHE), the quantum yield for charge injection to the semiconductor ($\phi$), and the efficiency of collecting electrons in the external circuit ($\eta$).[6][12]

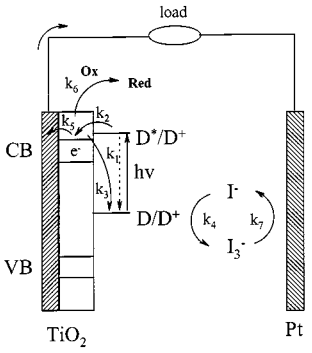


Scheme 1

$$IPCE = (LHE)(\Phi)(\eta) \qquad (1)$$

Several studies have focused on the role played by the different electron transfer processes in determining cell performances.[5,19−21] It has been shown that charge injection processes ($k_2$) take place in the femto- and/or picosecond time domain[8][22] with $\phi = 1$, and that an important factor decreasing the conversion efficiency is the electron transfer from the sensitized $TiO_2$ film to the relay electrolyte ($k_6$).[5] Recently, examples of the limiting role of iodide oxidation by oxidized dye ($k_4$) on the conversion efficiencies have been reported.[21]

The understanding of the key parameters affecting cell performances is of relevance to the design of the molecular sensitizer. A strong absorption in the visible part of the absorption spectrum is clearly beneficial. In addition, the excited-state properties and the redox potentials of the molecular dyes have to be tuned with respect to the level of the conduction band in the $TiO_2$ and to the redox potential of the sacrificial donor $I^-$, to increase the driving force of the corresponding electron transfer processes. The complexes which so far have shown the most promising characteristics, are based on ruthenium polypyridyl moieties incorporating

[a] Inorganic Chemistry Research Centre, School of Chemical Sciences,
Dublin City University, Dublin 9, Ireland
[b] Present address: Department of Chemistry, Dublin Institute of Technology,
Kevin Street, Dublin 8, Ireland
[c] Dipartimento di Chimica, Università di Ferrara,
Via L. Borsari N. 46, I-44100 Ferrara, Italy

  1434−1948/99/1212−2309 $ 17.50+.50/0 

negative monodentate ligands such as $NCS^-$.[6,10,16,23] The presence of monodentate ancillary ligands can, however, lead to some photochemical instability of the dye molecule which, in principle, can be reduced by using chelating ligands. We have therefore started a systematic investigation of potential dyes based upon triazole-type ligands.

Mixed-ligand $Ru^{II}$ complexes with electron rich 1,2,4-triazole-and 2,2′-bipyridine (bpy) containing ligands have been investigated in detail. Upon coordination the triazole ring is deprotonated, leaving a negative charge on the triazole ligand. It is well established that for complexes incorporating deprotonated triazole ligands the excited state is localized on the bpy moieties.[24−33]

In this study, the synthesis and characterization of complexes of the type $[Ru(dcb)_2(L)]$ {L = 3-(2-hydroxyphenyl)-5-(pyridin-2-yl)-1,2,4-triazole (2-ppt), 3-(4-hydroxyphenyl)-5-(pyridin-2-yl)-1,2,4-triazole (4-ppt), 3,5-bis(pyrazin-2-yl)-1,2,4-triazole (bpzt), 3-(2-hydroxyphenyl)-5-(pyrazin-2-yl)-1,2,4-triazole (2-ppzt); dcb = 4,4′-$(CO_2H)_2$-2,2′-bipyridine} is reported. The general structure of the complexes and ligands are depicted in Figure 1. The excited-state properties of the complexes in solution and when immobilized on $TiO_2$ have also been investigated by means of laser flash photolysis. The efficiency of the complexes as dyes in regenerative photoelectrochemical cells has been assessed and rationalized on the basis of an analytical expression correlating the IPCE to the relevant kinetic parameters schematized in Scheme 1.

## Results

### Electronic Absorption Spectra in Solution

Figure 2 shows the UV-Vis spectra of the complexes $[Ru(dcb)_2(L)]$ (L = 4-ppt, 2-ppt, bpzt or 2-ppzt) in aqueous solution at pH 7 (see also Table 1). At this pH both the triazole and dcb ligands are deprotonated (see discussion). The UV-Vis spectra for the complexes with 4-ppt or 2-ppt are nearly identical. The spectra obtained for the complexes containing the pyrazine-based ligands bptz and 2-ppzt are also very similar. The 4-ppt and 2-ppt complexes are characterized by absorption bands at 487, 437 and 367 nm, while the complexes containing bptz and 2-ppzt show a significant blue shift of the lowest energy absorption, with bands at about 461 and 433 nm. Lowering the pH to ca. 3 gives a characteristic blue shift for the 4-ppt and 2-ppt complexes, resulting in only two absorption bands each at 465, 433 and 473, 435 nm, respectively. The complexes with bpzt and 2-ppzt only showed band broadening. These changes are due to protonation of the triazole ring, and similar shifts have been observed for the corresponding mixed-ligand complexes containing bpy.[24−33] Decreasing the pH further resulted in precipitation of the compounds because of protonation of the carboxy ligands. The emission spectra were recorded in aqueous solution at pH 7, and the maxima are summarized in Table 1.

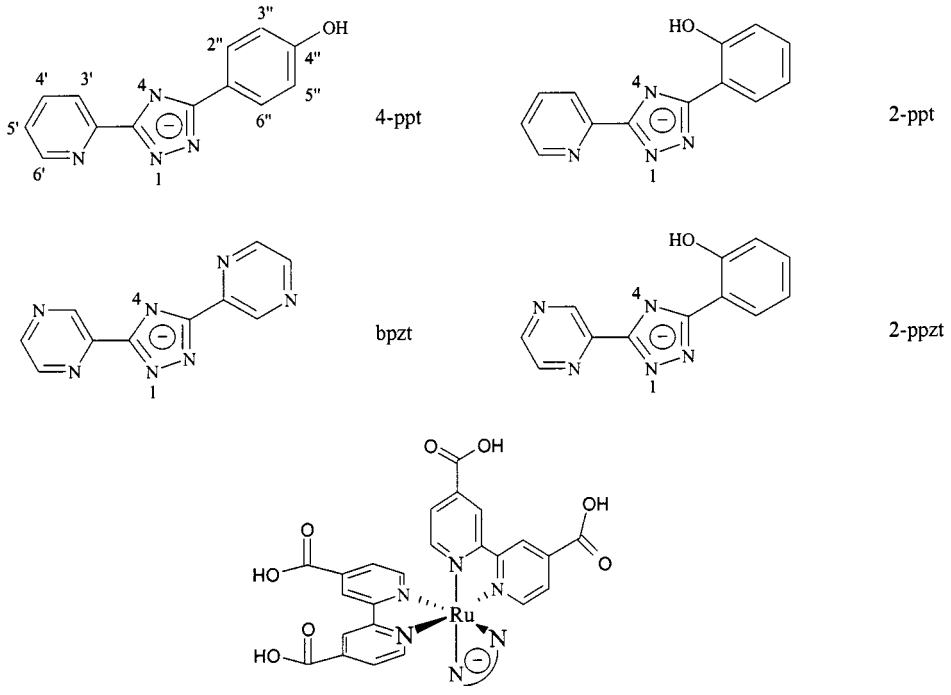


Figure 1. General molecular structure of $[Ru(H_2dcb)_2(L)]$ and the ligands L = 4-ppt, 2-ppt, bpzt and 2-ppzt

Table 1. Optical and electrochemical properties of the complexes $[Ru(dcb)_2(L)]$ (L = 4-ppt, 2-ppt, bpzt or 2-ppzt)

| Solution $TiO_2$ L | $\lambda_{max}$ (nm)[a] | $\lambda_{em}$ (nm)[a] | $\tau$ (ns)[b] | $E_{ox}$[c] | $\lambda_{max}$ (nm)[d] |
|---|---|---|---|---|---|
| 4-ppt | 487 | 691 | 40 | 1.02 | 495 |
| 2-ppt | 486 | 681 | 60 | | 495 |
| bpzt | 460 | 665 | 45 | 1.10 | 475 |
| 2-ppzt | 461 | 701 | 30 | 1.06 | 475 |

[a] $H_2O/Na_2CO_3$ at pH 7. – [b] Obtained from emission and transient-absorption difference spectra in degassed $H_2O/Na_2CO_3$ at pH 7 (estimated error ± 5 ns). – [c] Measured in DMF/0.1 M $LiClO_4$. – [d] Measured in MeCN.

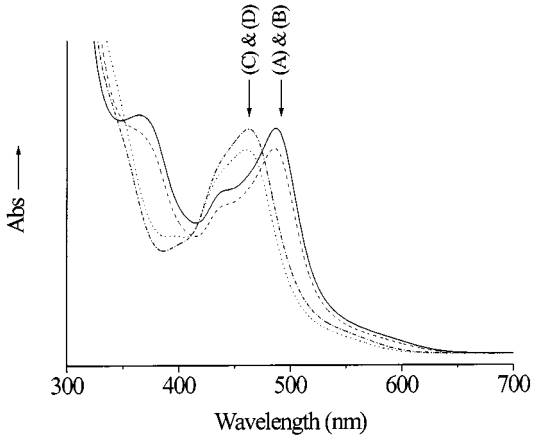


Figure 2. UV-Vis absorption spectra of (A) $[Ru(dcb)_2(4\text{-ppt})]$ (–), (B) $[Ru(dcb)_2(2\text{-ppt})]$ (- - -), (C) $[Ru(dcb)_2(bptz)]$ (···) and (D) $[Ru(dcb)_2(2\text{-ppzt})]$ (-·-·-) in aqueous solution at pH 7 (room temp.)

## Electrochemistry in Solution

The electrochemical properties of the complexes were measured in DMF/0.1 M $LiClO_4$. The redox potentials obtained are listed in Table 1. For the complexes $[Ru(dcb)_2(L)]$ (L = 4-ppt, 2-ppt or 2-ppzt) the voltamograms are complicated by the irreversible oxidation of the phenol ligand at about 1.3 V vs SCE. By comparison with data observed for the corresponding bpy complexes, the quasi reversible process at about 1 V vs Ag/AgCl can be assigned to the $Ru^{II}/Ru^{III}$ redox couple. The dcb-based reduction processes are irreversible. As observed before for other triazole-based ruthenium polypyridyl complexes, partial protonation of the triazole ring is observed when the potential is first cycled through the bpy-based reductions. In that case an additional redox wave at about 1.3 V is observed.[34]

## Photophysics in Solution

Flash photolysis experiments were carried out in degassed aqueous solution at pH 7, employing a 532 nm excitation pulse (6.5 mJ). The transient-absorption difference spectra of the complexes are shown in Figure 3. The spectra are characterized by a bleaching process in the 400–500 nm region and the formation of a new transition in the 350–400 nm region. The excited-state lifetime obtained from the transient spectra were identical to the lifetimes obtained from independent time-resolved emission measurements. The decay of the emission intensity was, in all cases, single exponential. The lifetimes of the various complexes are summarized in Table 1.

## Absorption spectra on $TiO_2$

The complexes $[Ru(dcb)_2(L)]$ were absorbed as a monolayer onto a ca. 7 μm thick nanocrystalline $TiO_2$ film. The UV-Vis spectra of two complexes (L = 2-ppt or bptz) on a $TiO_2$ film are shown in Figure 4. The absorption spectrum of $[Ru(dcb)_2(2\text{-ppt})]/TiO_2$ is mainly a superposition of the complex and the $TiO_2$. The absorption spectrum of the corresponding bpzt complex closely resembles the absorption spectrum in solution, but with different intensities of the absorption maxima. At 491 nm (2-ppt) and 475 nm (bptz) the absorbances were 1.60 and 1.84, respectively. Using the extinction coefficients at this wavelength, $1.0 \times 10^4$ $M^{-1}\cdot cm^{-1}$ (2-ppt) and $1.4 \times 10^4$ $M^{-1}\cdot cm^{-1}$ (bpzt),[25][35] and considering for the surface requirement of one adsorbed molecule the value of 100 Å$^2$, for a complete monolayer coverage, an average roughness factor of ca. 800 can be calculated.

## Photoelectrochemistry

The dye-molecules were tested in a standard photovoltaic cell (see experimental). Figure 5 shows a plot of the incident-photon-to-current efficiency (uncorrected for light absorption by the conductive glass) *vs.* the excitation wavelength, IPCE(λ), for the complexes. The IPCE(λ) is defined by Equation (2).[6][10]

Figure 5 demonstrates that the IPCE(λ) closely resembles the absorption spectra of the dye molecules attached to the $TiO_2$.

$$IPCE(\lambda) = \frac{1.24\ (eV\cdot nm)\ x\ photocurrentdensity\ (\mu A\cdot cm^{-2})}{wavelength\ (nm)\ x\ photonflux\ (\mu W\cdot cm^{-2})} \qquad (2)$$

## Photophysics on $TiO_2$

The transient-absorption difference spectra of the complexes $[Ru(dcb)_2(L)]$ anchored to $TiO_2$ are shown in Figure 6. The striking difference with the spectra recorded in solution (Figure 3) is the lack of the absorption band in the 350–400 nm region. The time-resolved absorbance changes of the complexes measured at 480 nm are depicted in Figure 7 [traces marked with **(1)**].

The traces were obtained by excitation with P = 0.3 $mJ\cdot cm^{-2}$. The back electron transfer between the electrons in the $TiO_2$ particle and the $Ru^{III}$ centers typically takes place in the nano- and microsecond time domain and is power dependent. At low excitation power, the back electron transfer is slower than at excitation with higher powers

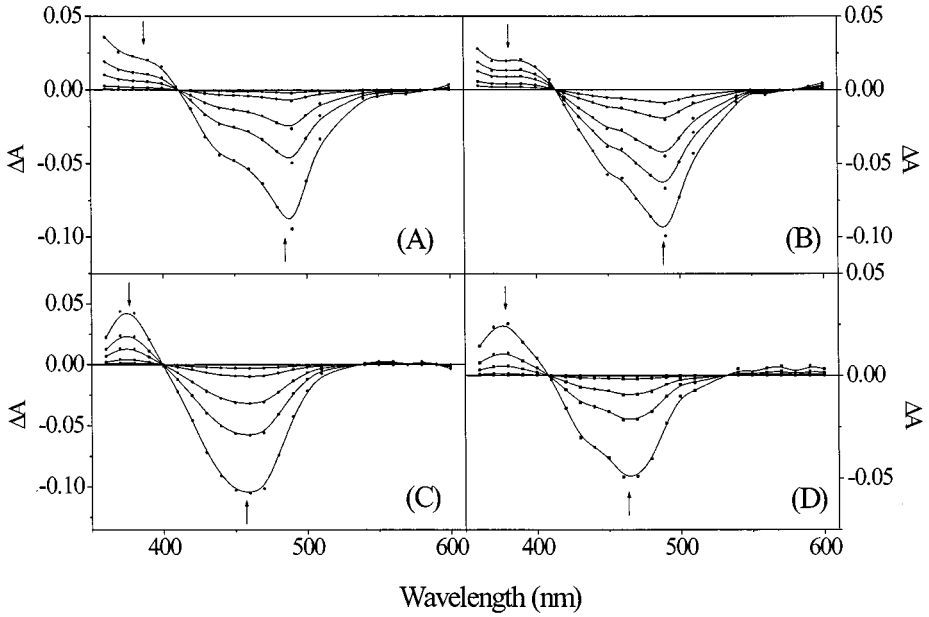


Figure 3. Time-resolved transient-absorption spectra in aqueous solution (pH 7; room temp.) of (A) $[Ru(dcb)_2(4\text{-ppt})]$, (B) $[Ru(dcb)_2(2\text{-ppt})]$, (C) $[Ru(dcb)_2(bpzt)]$ and (D) $[Ru(dcb)_2(2\text{-ppzt})]$ at $\tau_d$ = 0, 25, 50, 100 and 150 ns, respectively ($\lambda_{exc}$ = 532 nm, P = 6.5 mJ/Pulse)

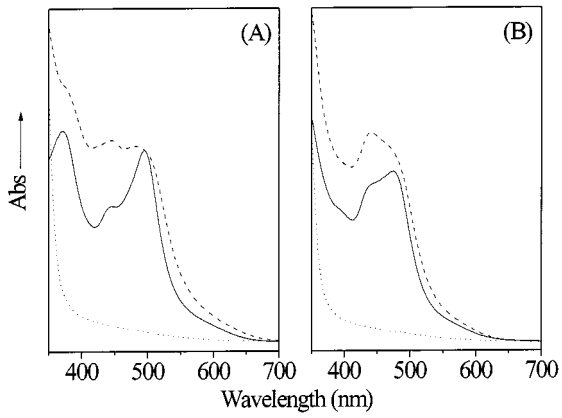


Figure 4. UV-Vis absorption spectra of (A) $[Ru(dcb)_2(2\text{-ppt})]$ (−), $[Ru(dcb)_2(2\text{-ppt})]/TiO_2$ (- - -) and $TiO_2$ (···) in MeCN (room temp.) (B) $[Ru(dcb)_2(2\text{-bpzt})]$ (−), $[Ru(dcb)_2(2\text{-bpzt})]/TiO_2$ (- - -) and $TiO_2$ (···) in MeCN (room temp.)

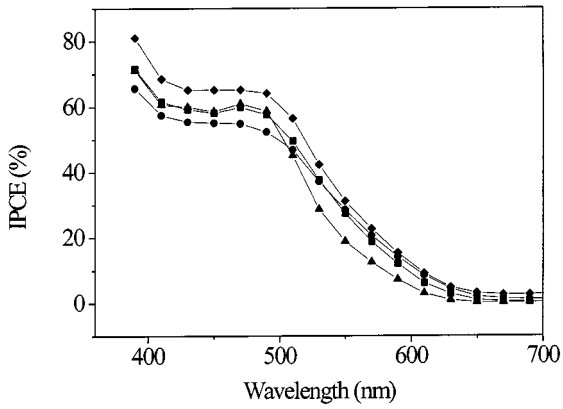


Figure 5. Incident photon-to-current efficiency *vs.* the excitation wavelength, IPCE(λ), for (▲) = $[Ru(dcb)_2(4\text{-ppt})]$, (■) = $[Ru(dcb)_2(2\text{-ppt})]$, (◆) = $[Ru(dcb)_2(bpzt)]$ and (●) = $[Ru(dcb)_2(2\text{-ppzt})]$

(spectra not shown). A detailed study[36] and description of the complexes kinetics is beyond the scope of this paper.

In order to get a better insight into the processes determining the efficiency of the photovoltaic cell, experiments in the presence of $I^-$ were employed. The quenching of oxidized dye molecules by 0.3 M $I^-$, giving rise to the parent complex, the iodine radical[19] and $TiO_2$-nanoparticle with an electron excess, are depicted in Figure 7 [traces marked with (2)]. The concentration of $I^-$ was the same as in a typical photovoltaic cell (0.3 M LiI) and the $Li^+$ concentration was kept constant with respect to the recombination experiments (0.3 M $LiClO_4$). The transient-absorption difference spectra in the presence of $I^-$ show a broad band (360−450 nm), most probably due to radical products of $I^-$ (spectrum not shown).[19] The quenching of $[Ru^{III}(dcb)_2(NCS)_2]$ by $I^-$ was observed to take place in the laser pulse (< 10 ns), while, under the same experimental conditions, the quenching of all $[Ru^{III}(dcb)_2(L)]$ dye molecules was slower and completed within ca. 100 ns.

## Discussion

In metal complexes with the triazole ligands reported here, the coordination mode of the triazole ring has to be considered. As Figure 1 shows, coordination of the triazole ring can occur through the N1 or the N4 atom. HPLC analysis of the reaction products shows that only one major product is obtained. It has been shown in the past that proton NMR spectroscopy can be used to determine the coordination mode of these ligands.[31−33,35,37,38] The spectra obtained for the compounds strongly indicate that for all compounds coordination of the triazole ring is through the N1 atom. N1 coordination is also to be expected from steric considerations. It is also important to note that the spectra

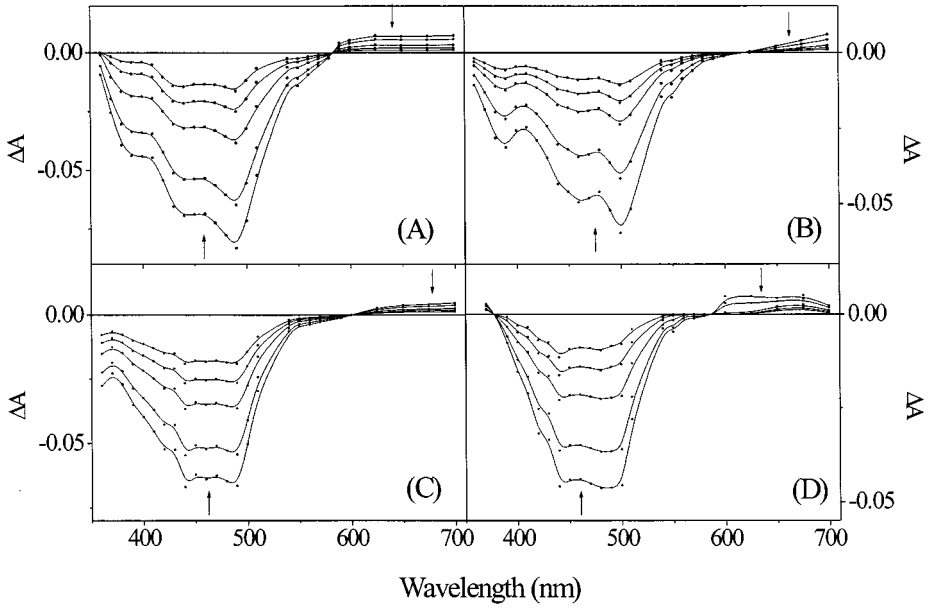


Figure 6. Time-resolved transient-absorption spectra of the $TiO_2$ films in MeCN/0.1 M $LiClO_4$ (room temp.), covered with (A) [Ru(dcb)$_2$(4-ppt)], (B) [Ru(dcb)$_2$(2-ppt)], (C) [Ru(dcb)$_2$(bpzt)] and (D) [Ru(dcb)$_2$(2-ppzt)] at $\tau_d$ = 0, 50, 250, 1000 and 2000 ns, respectively ($\lambda_{exc}$ = 532 nm, P = 0.5 mJ·cm$^{-2}$)

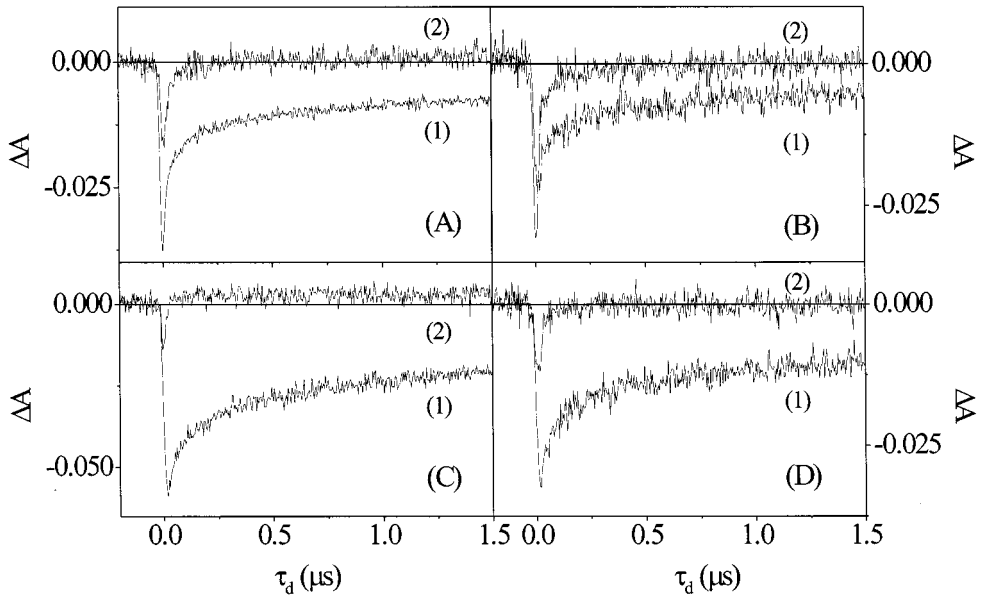


Figure 7. The microsecond decay kinetics measured at 480 nm of (A) [Ru(dcb)$_2$(4-ppt)], (B) [Ru(dcb)$_2$(2-ppt)], (C) [Ru(Hdcb)$_2$(bpzt)] and (D) [Ru(dcb)$_2$ (2-ppzt)] measured in the presence of (1) MeCN/0.3 M $LiClO_4$ and (2) MeCN/0.3 M LiI, respectively ($\lambda_{exc}$ = 532 nm, P = 0.3 mJ·cm$^{-2}$)

are recorded in DMSO/NaOD and, therefore, under these conditions, the complexes are completely deprotonated. The overall charge of the complexes is then 3−.

Intrinsically, the complexes reported here have very complicated acid-base properties. First of all the deprotonation steps of the dcb ligand have to be considered. The ligand shows two protonation steps for the complexes [Ru(bpy)$_{3-n}$(dcb)$_n$] ($n$ = 1,2,3) with p$K_{a2}$ values around 1.7−1.75 and p$K_{a1}$ values between 2.2−2.85.[39−42] For the excited states a p$K_a$*$_2$ value of 1.75 was estimated, while the p$K_a$*$_1$ value was found to increase from the corresponding ground-state value to between 4.6−4.25.[39−42] Secondly, the triazole ligands have their own acid-base properties. The ground-state p$K_a$ values for the closely related triazole complexes are between 2.0 and 5.5.[25,31−33,35,37,38] The pyridyltriazole-containing complexes are slightly more acidic in the excited state than in the ground state.[31][32] This is in agreement with resonance Raman, time-resolved resonance Raman, and excited-state absorption studies, which all support an excited state localized on the bpy ligands and triazole ligands that do not actively participate in the lowest excited state of the compounds.[24,26,27] For pyrazinetriazoles the

situation is even more complicated. The acid-base chemistry of these compounds together with resonance Raman data strongly suggest that when the triazole moiety is deprotonated (with a $pK_a$ of about 2.0) the excited state is based on the bpy ligand, while in complexes where protonation of the triazole ring has occurred the lowest energy excited state is based upon the pyrazine ring.[24][34] Furthermore, the complexes with 4-ppt, 2-ppt or 2-ppzt have a phenol group with a $pK_a$ of about 11.[25] These intricate acid-base properties make it impossible to isolate solid materials with a well-defined state of protonation. However, in solution under pH control, well-defined species are obtained as is shown in the NMR and UV-Vis spectra. For this reason we have used the $[Ru(dcb)_2(L)]$ formula to describe the solid complexes. All the photophysical measurements have been carried out under conditions where the triazole moiety is deprotonated. This ensures that the lowest energy excited state is based on the dcb ligands. This is also the case for the pyrazine based systems.

Analogous to the corresponding bpy complexes, the lowest absorption bands at ca. 470 nm, can be assigned to MLCT transitions between the metal and the dcb ligands. The complexes with the pyridine-based ligands 4-ppt and 2-ppt show MLCT bands at lower energy than those observed for the pyrazine-containing complexes. Since the lowest MLCT transitions originate from the $d_{Ru} \rightarrow \pi^*_{dcb}$ orbitals,[24] the observed red-shift for the pyridine-based complexes can be explained by the stronger σ-donor effect of the pyridine ring, resulting in an increase in energy of the d-orbitals of the metal center.[35] The UV-Vis spectra of the $Ru(dcb)_2$ pyridyltriazoles measured in aqueous solution at pH 7, where both the triazole and the polypyridyl ligands are deprotonated, show the same spectral properties as those of the corresponding $[Ru(bpy)_2(2\text{-ppt})]$ complex.[30] The spectral features of the $Ru(dcb)_2$ pyrazinetriazole compounds are similar to the spectra of $[Ru(bpy)_2(bpzt)]^+$.[33][35] All the absorption spectra show a typical red-shift of ca. 15−20 nm on going from bpy to dcb.[39][41] Under these circumstances, at pH 7, the emission maxima of the complexes are found at ca. 680 nm, which is a red-shift of 20 nm with respect to the values observed for the bpy derivatives, further supporting the proposition that the excited state is localized exclusively on the dcb ligand. The spectral changes observed on changing the pH to 3 correspond to the protonation of the triazole and dcb ligands.[30−33,35,37−42] An extensive study of the protonation behavior of the compound was not possible because further decreasing of the pH results in precipitation of the complexes.

The transient-absorption difference spectra of the $[Ru(dcb)_2(L)]$ complexes in aqueous solution (pH 7) show a bleach in the region 400−500 nm. This can be attributed to the disappearance of the MLCT transitions in the excited state. The strong absorption in the region 350−400 nm can be assigned to intraligand transitions of the dcb radical-anion. This behavior is typical for those Ru-complexes with a bpy/dcb ligand-localized excited state.[43−45] A comparable spectrum was found for $[Ru(bpy)_2(bpzt)]^+$.[24] The lifetimes of the excited states of the various complexes are in the range of 30−60 ns (see Table 1), which is shorter than the lifetimes observed for the corresponding bpy complexes, i.e. $[Ru(bpy)_2(bpzt)]^+$ (290 ns) and $[Ru(dcb)_2(bpzt)]$ (45 ns).[24] A red-shift of the absorption and emission maxima leads, in general, according to the energy gap law, to a decrease in lifetime.[46−48]

The complexes were absorbed on $TiO_2$ for photoelectrochemical measurements. Figure 4 shows that the optical properties of the dye molecules bound to $TiO_2$ and in solution (at pH 7) are comparable. The spectra also show that the triazole ligands are in the deprotonated form. The photoaction spectra (Figure 5 and Table 2) indicate that the complexes act as efficient sensitizers with $IPCE_{470nm}$ in the range 0.55−0.65 (0.68−0.80; values corrected for light absorption by the ITO glass). The fact that under similar experimental conditions the $[Ru(dcb)_2(NCS)_2]$ complex was shown to give better performances [$IPCE_{500nm} = 0.77$ (0.95; value corrected for light absorption by the ITO glass)] was unexpected, since the ground- and excited-state redox properties of these species are very similar. As shown in Equation 1, IPCE depends on the three terms $\Phi$ **(i)**, LHE **(ii)**, and $\eta$ **(iii)**, [6][12] which will be discussed separately:

**(i)** The absence of $^3[Ru(dcb)_2(L)]^*$ in the transient-absorption spectra of the dye on $TiO_2$, clearly shows that electron injection to the semiconductor is efficient (>95%) and takes place within the laser pulse (< 10 ns) or faster, which is in agreement with earlier reported data.[8][22]

**(ii)** Under the experimental conditions used, the LHE term for $[Ru(dcb)_2(NCS)_2]$ and the $[Ru(dcb)_2(L)]$ (L = 2-ppt, bpzt or 2-ppzt) complexes are the same, since for the examined photoanodes the incident light absorption was in the range 0.96−0.99 (see Table 2). Due to the low solubility of $[Ru(dcb)_2(4\text{-ppt})]$, the surface coverage on $TiO_2$ of the latter complex was lower than the other compounds, resulting in LHE = 0.90.

**(iii)** Significant differences are found for the quenching rate of $Ru^{III}$ by $I^-$ ($k_4$). For $[Ru(dcb)_2(NCS)_2]$ this process takes place in the laser pulse (less than 10 ns), while the quenching of $[Ru^{III}(dcb)_2(L)]$ is completed within less than 100 ns. The quenching of $[Ru^{III}(dcb)_2(bpzt)]$ by $I^-$ [Figure 7 (C) trace (2)] is completed in 30 ns, resulting in the highest IPCE value. The reaction of the $[Ru^{III}(dcb)_2(L)]$ (L = 4-ppt, 2-ppt or 2-ppzt) with $I^-$ is slower (100 ns), resulting in lower IPCE values. Furthermore, one should realize that any formation of $Ru^{III}$ in the presence of $I^-$ directly leads to losses in efficiency. Apparently, the quenching rate of $Ru^{III}$ by $I^-$ is an important parameter in the efficiency of the photovoltaic cell. Differences in IPCE values, therefore, most likely reflect a variation in η values, which reflects the processes $k_3$, $k_4$ and $k_5$. The traces obtained from the quenching experiments [Figure 7 (C) trace (2)] do not give the rate constant ($k_4$) for the quenching of the $Ru^{III}$ by $I^-$.

$$S^+ + e^- \xrightarrow{k_3} S$$
$$S^+ + I^- \xrightarrow{k_4} S + I^{\bullet} \qquad (3)$$

$$[S^+] = [S^+]_0 e^{-(k_3+k_4)t} \qquad (4)$$

From Equations 3 and 4 it can easily be seen that the observed rate constant is the sum of the quenching rate constant ($k_4$) and the back electron transfer ($k_3$).

Analogous to the quantum yield of injection ($\Phi$), the efficiency of quenching (defined as) $\eta$, of $Ru^{III}$ by $I^-$ is described by Equation 5 or 6. These equations describe the interplay between the quenching of $Ru^{III}$ by $I^-$ ($k_4$) and the recombination of the electrons in the conduction band with the $Ru^{III}$ center ($k_3$). The appendix shows the full derivation for all the processes involved in the IPCE under steady-state conditions, resulting in the same terms for η if $k_6[e^-] << k_7[e^-_{ex}]$,[49−53]

$$\eta = \frac{k_4[I^-]}{k_3[e^-] + k_4[I^-]} \quad \text{or} \quad \eta = 1 - \frac{k_3[e^-]}{k_3[e^-] + k_4[I^-]} \qquad (5) \text{ and } (6)$$

$$\eta = \frac{k_4}{k_3 + k_4} \quad \text{or} \quad \eta = 1 - \frac{k_3}{k_3 + k_4} \qquad (7) \text{ and } (8)$$

Application of these formulae is not straightforward, since the experimental $k_3$ and ($k_3$ + $k_4$) are not first or second order. For the estimation of η, the simplified first order formulae (Equation 7 and 8) and the following parameters were used: (i) ($k_3$ + $k_4$) is equal to $k_{obs}$ in the $Ru^{III}$/$I^-$ quenching experiment (see Equations 3 and 4), and was treated as a single exponential; (ii) the traces of the recombination of the electron in $TiO_2$ with the oxidized dye molecule ($k_3$) can be fitted with a bi-exponential function (see Table 2), which indicates a fast component ($k \approx 1 \times 10^7$ $s^{-1}$ and a slow component ($k \approx 4 \times 10^5$ $s^{-1}$). Since the quenching of $Ru^{III}$ by $I^-$ is completed within 100 ns, only the fast exponential component of $k_3$ is considered. Using these rate constants and Equation 7 or 8 we calculated values for η (Table 2). For the steady-state measurements, η can be calculated (Table 2) from Equation 1, the LHE term and $\phi = 1$. The values for the η term obtained by this transient-absorption study are in good agreement with the values found in the steady-state experiments. As a consequence, the delicate interplay between the quenching of $Ru^{III}$ by $I^-$ ($k_4$) and the recombination of the electrons in the conduction band with the $Ru^{III}$ center ($k_3$) apparently determines the efficiency of a regenerative solar cell based on ruthenium dyes.

## Experimental Section

**Materials and Apparatus and Preparations:** [$RuCl_3 \cdot H_2O$] (Oxkem Ltd), 4,4′-dimethyl-2,2′-bipyridine (Aldrich) were used without further purification. The solvents for the spectroscopic measurements, acetonitrile (Aldrich), methanol (Aldrich) were of spectroscopic grade and were used as received. 4,4′-Dicarboxy-2,2′-bipyridine (dcb) was prepared by the method of Oki et al.[54] The ligands 4-ppt,[37] 2-ppt,[30] bpzt[35] and 2-ppzt[38] were prepared as previously described. The complexes [$Ru(dcb)_2Cl_2$] and [$Ru(dcb)_2(NCS)_2$] were prepared according to literature procedures.[55] UV-Vis spectra were recorded with a Kontron Uvikon 860 spectrophotometer. Emission spectra were measured on a SPEX Fluoromax 2 spectrofluorimeter equipped with a Hamamatsu R3896 tube. The emission spectra were corrected for the instrumental response. The NMR spectra were recorded on a Bruker AMX 400. HPLC was carried out on a Waters system equipped with a 990 photodiode array detector with a SAX anionic exchange column (8 × 100 mm) and 50:50 (MeCN/$H_2O$) 0.05 M phosphate buffer as the mobile phase. The $TiO_2$ films were prepared as described by Nazeeruddin et al.[6] For the IPCE measurement the $TiO_2$ was deposited on conductive fluorine-doped $SnO_2$ glass (LOF ≈ 10Ω/□), while for the transient-absorption measurement normal glass was used. The films were heated at 450°C for 30 min. Coating of the $TiO_2$ surface with the dye was carried out by soaking the film for 3 h (transient-absorption experiments) and 24 h (IPCE measurements) in a ca. $1 \times 10^{-4}$ M methanol solution of the complexes. After completion of the dye adsorption, the film was rinsed with acetone and dried (10 min. at 60°C). The measurements were performed directly after the preparation of the film. The complexes [$Ru(dcb)_2(L)$] (L = 4-ppt, 2-ppt, bpzt or 2-ppzt) were stable towards daylight and oxygen in methanol solution as well as when bound to the $TiO_2$ surface. Photoelectrochemical measurements were performed in a two-electrode sandwich cell arrangement by using $SnO_2/TiO_2$/dye as the photoanode (active area 0.5 $cm^2$) and a $SnO_2$/Pt-coated glass as counterelectrode. The sandwich cell was filled with an acetonitrile solution containing 0.3 M LiI and 0.03 M $I_2$. The current measurements were performed with a Kontron DDM4021 Digital Multimeter. The excitation source was a 150 W Xe lamp coupled to a 0.22 m monochromator. Incident light flux was measured with a UDT-calibrated Si-diode. In order to minimize errors in the IPCE measurements, the complexes and [$Ru(dcb)_2(NCS)_2$] are measured in at least two different cells, resulting in an estimated error of 5%. Nanosecond flash photolysis transient-absorption spectra were measured by irradiating the sample with 6−8 ns (fwhm) of a Continuum Surelight Nd:Yag laser (10 Hz repetition rate) and using as probe light a pulsed Xe-lamp perpendicular to the laser beam. The excitation wavelength was

Table 2. Parameters from the time resolved and steady state experiments for the determination of the η term

| L | Time-resolved $k_3$[a] × $10^6$ | Steady-state $k_3 + k_4$[b] × $10^6$ | $\eta_{calc}$[c] | $IPCE_{470nm}$ | $LHE_{470nm}$[d] | $\eta_{calc}$[e] |
|---|---|---|---|---|---|---|
| 4-ppt | 14.7(55%) 0.4(45%) | 66.7 | 0.78 | 0.74 | 0.90 | 0.82 |
| 2-ppt | 11.6(55%) 0.4(45%) | 62.5 | 0.81 | 0.73 | 0.97 | 0.75 |
| bpzt | 8.5(43%) 0.3(57%) | 71.4 | 0.88 | 0.80 | 0.98 | 0.82 |
| 2-ppzt | 8.8(49%) 0.3(51%) | 38.4 | 0.77 | 0.68 | 0.99 | 0.69 |

[a] Kinetic data from the traces (1) of Figure 7. − [b] Kinetic data from the traces (2) of Figure 7, $k_{obs} = k_3 + k_4$. − [c] Calculated from Equation 8. − [d] LHE = $1-10^{-A}$, where A is the absorbance of the dye on the $TiO_2$ layer, see also ref.[6][12] − [e] Calculated from Equation 1, with $\phi = 1$.

obtained by frequency doubling (532 nm). The 150 W Xe lamp was equipped with an Applied Photophysics Model 408 power supply and Applied Photophysics Model 410 pulsing unit (giving pulses of 0.5 ms). A shutter, Oriel Model 71445, placed between the lamp and the sample was opened for 100 ms to prevent PMT fatigue. Suitable pre- and post-cutoff and bandpass filters were used to minimize the probe light and scatter light of the laser. The films were oriented at 45° to the laser and probe light and set up in such a way that the scattered light was reflected to the probe light. In this way we were also able to measure in the early time domain (t < 50 ns) without registering artifacts due to scattered light. The sampling rate was kept at a relatively long time (intervals of 10 s) to prevent electron accumulation in the conduction band of the semiconductor. The light was collected in a LDC Analytical monochromator, detected by a R928 PMT (Hamamatsu), and recorded on LeCroy 9360 (600 MHz) oscilloscope. The laser oscillator, Q-switch, lamp, shutter and trigger were externally controlled with a digital logic circuit, which allowed synchronous timing. The absorption transients were plotted as $\Delta A = \log(I_o/I_t)$ *vs* time, where $I_o$ was the monitoring light intensity prior to the laser pulse and $I_t$ was the observed signal at delay time $t$. The same setup as described above was employed for the time-resolved emission experiments, with the exception that the probe lamp was not used.

**Synthesis of Metal Complexes:** The complexes containing the triazole ligands were prepared by the following procedure. The ligand ($4 \times 10^{-4}$ M) was heated under reflux in a basic solution of 2:1 ethanol/water (ca. 20 mL) to which the $[Ru(dcb)_2Cl_2]$ ($3.2 \times 10^{-4}$ M) was added. The mixture was further heated at reflux for 3−4 h and the reaction was monitored by HPLC. The product was precipitated by lowering the pH to 2.7 with HCl (ca. 2 mL, 0.2 M) and purified after resolution in water at pH 7 by column chromatography with Sephadex LH20 resin. Isolation of the product after chromatography was achieved by adjusting the pH with HCl as before. In the molecular formulas given below, the degree of protonation and therefore the charge of the complexes has not been defined. Protonation is strongly dependent on the pH of the solution and the $pK_a$ values of the various ligands. The materials obtained have been characterized by proton NMR and anion exchange HPLC.

**[Ru(dcb)$_2$(4-ppt)]:** $^1$H NMR ([D$_6$]DMSO/NaOD, 293 K) δ = 8.80−8.76 (d, 4 H, dcb-H$_6$), 8.15 (d, 1 H, H$_{3'}$), 7.92 (t, 1 H, H$_{4'}$), 7.79 (d, 1 H, H$_{6''}$), 7.67 (d, 1 H, H$_{2''}$), 7.74−7.66 (m, 8 H, dcb-H$_3$ and dcb-H$_5$) 7.41 (d, 1 H, H$_{6'}$), 7.20 (t, 1 H, H$_{5'}$), 6.71 (d, 2 H, H$_{3''}$ and H$_{5''}$). − UV/Vis (aqueous solution pH 7): $\lambda_{max}$ = 487, 437, 367. − Yield 60%.

**[Ru(dcb)$_2$(2-ppt)]:** $^1$H NMR ([D$_6$]DMSO/NaOD, 293 K) δ = 8.93−8.89 (d, 4 H, dcb-H$_6$), 8.20 (d, 1 H, H$_{3'}$), 8.01 (t, 1 H, H$_{4'}$), 7.93 (d, 1 H, H$_{6''}$), 7.89−7.71 (m, 8 H, dcb-H$_3$ and dcb H$_5$), 7.53 (d, 1 H, H$_{6'}$), 7.31 (t, 1 H, H$_{5'}$), 7.15 (t, 1 H, H$_{4''}$), 6.83−6.79 (m, 2 H, H$_{5''}$ and H$_{3''}$). − UV/Vis (aqueous solution pH 7): λ = 486, 436, 367. − Yield 65%.

**[Ru(dcb)$_2$(bpzt)]:** $^1$H NMR ([D$_6$]DMSO/NaOD 293 K) δ = 9.30 (s, 1 H, H$_{3'}$), 9.05 (s, 1 H, H$_{6''}$), 8.75 (d, 4 H, dcb-H$_6$), 8.56 (d, 1 H, H$_{3''}$), 8.46 (d, 1 H, H$_{4''}$), 8.28 (d, 1 H, H$_{6'}$), 7.90−7.61 (m, 8 H, dcb-H$_3$ and dcb-H$_5$), 7.64 (d, 1 H, H$_{5'}$). − UV/Vis (aqueous solution pH 7): λ 461, 433. − **[Ru(dcbH$_2$)$_2$(Hbpzt)]Cl$_2$**·4 H$_2$O: $C_{34}H_{31}Cl_2N_{11}O_{12}Ru$ (957.7): calcd. C 42, N 16.08, H 3.23; found C 42.60, N 15.89, H 3.08. − Yield 75%.

**[Ru(dcb)$_2$(2-ppzt)]:** $^1$H NMR ([D$_6$]DMSO/NaOD, 293 K) δ = 9.39 (s, 1 H, H$_{3'}$), 8.79 (d, 4 H, dcb-H$_6$), 8.22 (d, 1 H, H$_{5'}$), 7.88 (d, 1 H, H$_{6''}$), 7.72−7.57 and 7.36−7.34 (m, 8 H, dcb-H$_3$ and dcb-H$_5$), 7.54 (d, 1 H, H$_{6'}$), 6.78 (t, 1 H, H$_{4''}$), 6.40 (d, 1 H, H$_{3''}$), 6.05 (t, 1 H, H$_{5''}$). − UV/Vis (aqueous solution pH 7): $\lambda_{max}$ = 462, 433 nm. − Yield 60%.

## Appendix

According to Scheme 1, the following chemical reactions can be summarized:

$$S \xrightarrow{h\nu,\phi} S^+ + e^-$$
$$S^+ + e^- \xrightarrow{k_3} S$$
$$S^+ + I^- \xrightarrow{k_4} S + I^\bullet$$
$$e^- \xrightarrow{k_5} e^-_{ex}$$
$$e^- + I^\bullet \xrightarrow{k_6} I^-$$
$$e^-_{ex} + I^\bullet \xrightarrow{k_7} I^-$$

Under steady-state conditions of for $[S^+]$,$[I^\bullet]$, and$[e^-]$ follows:

$$(A.1) \quad \frac{\partial[S^+]}{\partial t} = \phi I_{abs} - k_3[S^+][e^-] - k_4[S^+][I^-] = 0$$

$$(A.2) \quad [S^+] = \frac{\phi I_{abs}}{k_3[e^-] + k_4[I^-]}$$

$$(A.3) \quad \frac{\partial[I^\bullet]}{\partial t} = k_4[S^+][I^-] - k_6[I^\bullet][e^-] - k_7[I^\bullet][e^-_{ex}] = 0$$

$$(A.4) \quad [I^\bullet] = \frac{k_4[S^+][I^-]}{k_6[e^-] + k_7[e^-_{ex}]}$$

$$(A.5) \quad \frac{\partial[e^-]}{\partial t} = \phi I_{abs} - k_3[S^+][e^-] - k_5[e^-] - k_6[I^\bullet][e^-] = 0$$

Substitution of (A.2) and (A.4) in (A.5), with $J_{ex} = k_5[e^-]$, results in:

$$(A.6) \quad J_{ex} = \phi I_{abs}\left(\frac{k_4[I^-]}{k_3[e^-] + k_4[I^-]} \cdot \frac{k_7[e^-_{ex}]}{k_6[e^-] + k_7[e^-_{ex}]}\right)$$

Since $I_{abs} = I_o(LHE)$, (A.6) becomes:

$$(A.7) \quad IPCE = \frac{J_{ex}}{I_0} = (LHE)(\phi)(\eta) \text{ with } \eta = \left(\frac{k_4[I^-]}{k_3[e^-] + k_4[I^-]} \cdot \frac{k_7[e^-_{ex}]}{k_6[e^-] + k_7[e^-_{ex}]}\right)$$

If $k_6[e^-] << k_7[e^-_{ex}]$ then $\eta$ can be written as:

$$(A.8) \quad \eta = \frac{k_4[I^-]}{k_3[e^-] + k_4[I^-]} \quad \text{or} \quad \eta = 1 - \frac{k_3[e^-]}{k_3[e^-] + k_4[I^-]}$$

## Acknowledgments

Financial support from TRM Grant CT96−0076 and JOULE JOR3-CT95−00107 is gratefully appreciated.

[1] B. O'Regan, M. Grätzel, *Nature* **1991**, *353,* 737.
[2] U. Back, D. Lupo, P. Comte, J. E. Moser, F. Weissörtel, J. Salbeck, H. Spreitzer, M. Grätzel, *Nature* **1998**, *395,* 583.
[3] A. Hagfeldt, M. Grätzel, *Chem. Rev.* **1995**, *95,* 49.
[4] N. J. Cherepy, G. P. Smestad, M. Grätzel, J. Z. Zhang, *J. Phys. Chem. B* **1997**, *101,* 942.
[5] S. Y. Huang, G. Schlichthörl, A. J. Nozik, M. Grätzel, A. J. Frank, *J. Phys. Chem. B* **1997**, *101,* 2576.
[6] M. K. Nazeeruddin, M. Kay, I. Rodicio, R. Humphry-Baker, E. Müller, P. Liska, N. Vlachopoulos, M. Grätzel, *J. Am. Chem. Soc.* **1993**, *115,* 6382.
[7] B. O'Regan, J. Moser, M. Anderson, M. Grätzel, *J. Phys. Chem.* **1990**, *94,* 8720.
[8] Y. Tachibana, J. E. Moser, M. Grätzel, D. R. Klug, J. R. Durrant, *J. Phys. Chem.* **1996**, *100,* 20056.
[9] T. A. Heimer, C. A. Bignozzi, G. J. Meyer, *J. Phys. Chem.* **1993**, *97,* 11987.
[10] R. Argazzi, C. A. Bignozzi, T. A. Heimer, F. N. Castellano, G. J. Meyer, *Inorg. Chem.* **1994**, *33,* 5741.

[11] R. Argazzi, C. A. Bignozzi, T. A. Heimer, N. Castellano, G. J. Meyer, *J. Phys. Chem. B* **1997**, *101,* 2591.
[12] C. A. Bignozzi, J. R. Schoonover, F. Scandola, *Molecular level artificial photosynthetic materials,* Vol. 44, Wiley, New York, **1997**.
[13] G. J. Meyer, *J. Chem. Educ.* **1997**, *74,* 652.
[14] S. G. Yan, A. Lyon, B. I. Lemon, J. S. Preiskorn, J. T. Hupp, *J. Chem. Educ.* **1997**, *74,* 657.
[15] G. Smestad, C. A. Bignozzi, R. Argazzi., *Sol. Energy Mater. Sol. Cells.* **1994**, *32,* 259.
[16] M. K. Nazeeruddin, P. Pèchy, M. Grätzel, *Chem. Commun.* **1997**, 1705.
[17] H. Gerischer, *Electrochim. Acta* **1990**, *35,* 1677.
[18] B. A. Parkinson, M. T. Splitler, *Electrochim. Acta* **1992**, *37,* 943 and references cited therein.
[19] C. Nasr, H. Surat, P. V. Kamat, *J. Phys. Chem. B* **1998**, *102,* 4944.
[20] R. Argazzi, C. A. Bignozzi, G. M. Hasselmann, G. J. Meyer, *Inorg. Chem.* **1998**, *37,* 4533.
[21] M. Alebbi, C. A. Bignozzi, T. A. Heimer, G. M. Hasselmann, G. J. Meyer, *J. Phys. Chem. B.* **1998**, *102,* 7577.
[22] T. Hannappel, B. Burfeindt, W. Storck, F. Willig, *J. Phys. Chem. B* **1997**, *1997,* 6799.
[23] O. Kohle, S. Ruile, M. Grätzel, *Inorg. Chem.* **1996**, *35,* 4779.
[24] C. G. Coates, T. E. Keyes, H. P. Hughes, P. M. Jayaweera, J. J. McGarvey, J. G. Vos, *J. Phys.Chem. A* **1998**, *102,* 5013.
[25] R. H. Hage, A. H. J. Dijkhuis, J. G. Haasnoot, R. Prins, J. Reedijk, B. E. Buchanan, J. G. Vos, *Inorg. Chem.* **1988**, *27,* 2185.
[26] H. A. Nieuwenhuis, J. G. Haasnoot, R. Hage, J. Reedijk, T. L. Snoeck, D. J. Stufkens, J. G. Vos, *Inorg. Chem.* **1991**, *30,* 48.
[27] H. P. Hughes, D. Martin, S. E. J. Bell, J. J. McGarvey, J. G. Vos, *Inorg. Chem.* **1993**, *32,* 4402.
[28] H. P. Hughes, J. G. Vos, *Inorg. Chem.* **1995**, *34,* 4001.
[29] T. E. Keyes, J. G. Vos, J. A. Kolnaar, J. G. Haasnoot, J. Reedijk, R. H. Hage, *Inorg. Chim. Acta* **1996**, 237.
[30] R. Hage, J. G. Haasnoot, J. Reedijk, R. Wang, E. M. Ryan, J. G. Vos, A. L. Spek, A. J. M. Duisenberg, *Inorg. Chim. Acta* **1990**, *174,* 77.
[31] R. Wang, J. G. Vos, R. H. Schmehl, R. Hage, *J. Am. Chem. Soc.* **1992**, *114,* 1964.
[32] B. E. Buchanan, J. G. Vos, W. J. M. van der Putten, J. M. Kelly, R. Hage, R. A. G. de Graaff, R. Prins, J. G. Haasnoot, J. Reedijk, *J. Chem. Soc., Dalton Trans.* **1990**, 2425.
[33] R. Hage, J. G. Haasnoot, H. A. Nieuwenhuis, J. Reedijk, R. Wang, J. G. Vos, *J. Chem. Soc., Dalton Trans.* **1991**, 3271.
[34] R. Hage, R. Prins, J. G. Haasnoot, J. Reedijk, J. G. Vos, *J. Chem. Soc., Dalton Trans.* **1987**, 1389.
[35] R. H. Hage, J. G. Haasnoot, J. Reedijk, R. Wang, J. G. Vos, *Inorg. Chem.* **1991**, *30,* 3263.
[36] C. J. Kleverlaan, to be published.
[37] T. E. Keyes, Ph.D. thesis, Dublin City University **1994**.
[38] B. Evrard, unpublished results .
[39] P. J. Giordano, C. R. Bock, M. S. Wrighton, L. V. Interrante, R. F. X. Williams, *J. Am. Chem. Soc.* **1977**, *99,* 3187.
[40] J. Ferguson, A. W. H. Mau, W. H. F. Sasse, *Chem. Phys. Lett.* **1979**, *68,* 21.
[41] M. D. Nazeeruddin, K. Kalyanasundaram, *Inorg. Chem.* **1989**, *28,* 4251.
[42] J. G. Vos, *Polyhedron* **1992**, *11,* 2285.
[43] P. S. Braterman, A. Harriman, G. A. Heath, L. Yellowless, *J. Chem. Soc., Dalton Trans.* **1983**, 1801.
[44] R. J. Watts, *J. Chem. Educ.* **1983**, *60,* 834.
[45] K. Kalyanasundaram, *Photochemistry of Polypyridine and Porphyrin Complexes*, Academic, New York, **1992**.
[46] E. M. Kober, J. V. Caspar, R. S. Lumpkin, T. J. Meyer, *J. Phys. Chem.* **1986**, *90,* 3722.
[47] K. R. Barqawi, A. Llobet, T. J. Meyer, *J. Am. Chem. Soc.* **1988**, *110,* 7751.
[48] K. R. Barqawi, Z. Murtaza, T. J. Meyer, *J. Phys. Chem.* **1991**, *95,* 47.
[49] Under steady-state conditions $k_5 = k_7$; the response time of a cell is typically in the ms time domain, see ref.[50–53].
[50] J. J. Kelly, D. Vanmaekelbergh, *Electrochim. Acta* **1998**, *43,* 2773.
[51] P. E. de Jongh, D. Vanmaekelbergh, *J. Phys. Chem. B* **1997**, *101,* 2716.
[52] F. Cao, G. Oskam, G. J. Meyer, P. C. Searson, *J. Phys. Chem.* **1996**, *100,* 17021.
[53] J. S. Salafsky, W. H. Lubberhuizen, E. van Faassen, R. E. I. Schropp, *J. Phys. Chem. B* **1998**, *102,* 766.
[54] A. R. Oki, R. J. Morgan, *Synth. Commun.* **1995**, *25,* 4093.
[55] P. Liska, N. Vlachopoulos, M. K. Nazeeruddin, P. Comte, M. Grätzel, *J. Am. Chem. Soc.* **1988**, *110,* 3687.

Received March 8, 1999
[I99091]